ROSE 2008 - IEEE International Workshop
on Robotic and Sensors Environments
Ottawa - Canada, 17-18 October 2008

An omnidirectional stereoscopic system for mobile robot navigation

R. Boutteau, X. Savatier, J.Y. Ertaud, B. Mazari

Research Institute for Embedded Systems (IRSEEM),
Technopole du Madrillet - Av. Galilée - BP10024
76801 Saint Etienne du Rouvray Cedex - France
E–mail: {boutteau, savatier, ertaud, mazari}@esigelec.fr.

Abstract – *This paper proposes a scheme for a 3D metric reconstruction of the environment of a mobile robot. We first introduce the advantages of a catadioptric stereovision sensor for autonomous navigation and how we have designed it with respect to the Single Viewpoint constraint. For applications such as path generation, the robot needs a metric reconstruction of its environment, so calibration of the sensor is required. After justification of the chosen model, a calibration method to obtain the model parameters and the relative pose of the two catadioptric sensors is presented. Knowledge of all the sensor parameters yields the 3D metric reconstruction of the environment by triangulation. Tools for calibration and relative pose estimation are presented and are available on the author's web page. The entire process has been evaluated using real data.*

Keywords – *omnidirectional sensor, calibration, stereovision.*

I. INTRODUCTION

Interest in autonomous robots has been growing over the past few years in many applications: intervention in hostile environments, preparation of military intervention, mapping, etc. In many case, the navigation should be done in an unknown environment and can be helped by 3D reconstruction.

Autonomous navigation requires a large field of view to provide a complete map of the environment. Therefore, interest for omnidirectional vision, which provides a 360-degree field of view, has consequently grown up significantly. To obtain a panoramic image, several methods are being explored: rotating cameras [1], multicamera systems and catadioptric sensors [2]. We chose to work on catadioptric sensors (camera/mirror combination) because they are able to provide a panoramic image instantaneously and without moving parts.

To achieve a 3D reconstruction, it is necessary to have two images of the environment from two different viewpoints either by moving a single camera or by using a multicamera system. The second way is more suitable for dynamic environments because it provides stereo-pair images instantaneously and the 3D reconstruction can be initialized without any motion.

Our work focuses on the development of a catadioptric stereovision sensor and of a complete toolchain, from calibration to 3D reconstruction.

The following section describes our catadioptric stereovision system and how we designed it to respect the Single View-Point constraint. Section III is devoted to the choice of the model. In section IV, we describe the calibration tool developed to determine the model parameters, while in section V we present the relative pose estimation of the two sensors. In section VI we explain how to obtain the 3D coordinates of points and our experimental results are shown in section VII. Finally, in sections VIII and IX, we draw some conclusions and establish future directions for research.

II. SENSOR DESCRIPTION

A. Sensor configuration

It is a well-known fact that a 360-degree field of view presents advantages for navigation since there are interesting optical flow properties [3] and more visual features to track. Although it is possible to reconstruct the environment with only one camera, a stereoscopic sensor can produce a 3D reconstruction instantaneously (without displacement) and will give better results in dynamic scenes.

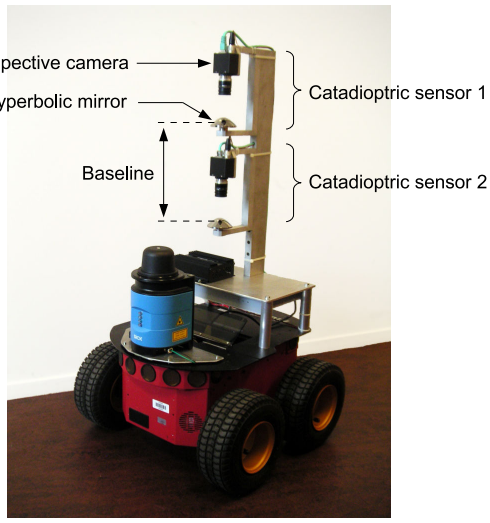

Fig. 1. View of our catadioptric stereovision sensor mounted on a Pioneer robot. Baseline is approximately 20cm for indoor environments and can be extended for outdoor environments. The overall height of the sensor is 40cm.

Among all possible configurations of central catadioptric sensors describes by [2], we have chosen to combine two hy-

perbolic mirrors with two cameras (see Fig. 1) for the sake of compactness (a parabolic mirror needs a bulky telecentric lens).

B. How to respect the Single-Viewpoint (SVP) constraint

The formation of images with catadioptric sensors is based on the Single-Viewpoint (SVP) theory [2]. When the Single-Viewpoint constraint is respected, sensed images are geometrically correct (pure perspective) and the epipolar geometry is applicable. In the case of a hyperbolic mirror (see Fig. 2), the optical center of the camera has to coincide with the second focus F' of the hyperbola located at a distance of $2e$ from the mirror focus. The eccentricity e is a parameter of the mirror given by the manufacturer.

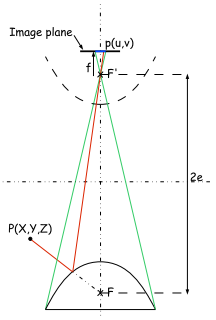

Fig. 2. Image formation with a hyperbolic mirror. The camera center has to be located at $2e$ from the mirror focus to respect the SVP constraint.

A key step in designing a catadioptric sensor is to respect this constraint as much as possible. To achieve this, we first calibrate our camera with a standard calibration tool such as that of J.Y. Bouguet [4] to determine the central point and the focal length. Knowing the parameters of both the mirror and the camera, the image of the mirror on the image plane can be easily predicted if the SVP constraint is respected (see Fig. 2). The expected mirror boundaries are drawn and the mirror has then to be moved to fit this estimation (see Fig. 3).

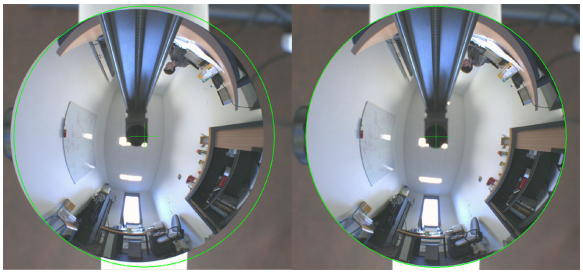

Fig. 3. Adjustment of the mirror position to respect the SVP constraint. The mirror border has to fit the estimation (green circle).

III. PROJECTION MODEL

The modelling of the sensor is a necessary step before 3D reconstruction can take place because it establishes the relation between the 3D points of the scene and their projections in the image (pixel coordinates). Although there are many calibration methods, they can be classified into two main categories: parametric and non-parametric. The first family consists in finding an appropriate model for the projection of a 3D point onto the image plane. Non-parametric methods associate one projection ray to each pixel [5], [6], and provide a "black box model" of the sensor. They are well adapted for general purposes but they restrict the number of suitable 3D reconstruction algorithms. We consequently chose a parametric calibration method. Using a parametric method requires the choice of the model, which is very important because it has an effect on the complexity and the precision of the calibration process. Several models are available for catadioptric sensors: complete model, polynomial approximation of the projection function and generic model.

The complete model relies on the mirror equation, the camera parameters and the rigid transformation between them to calculate the projection function [7]. The large number of parameters to be estimated leads to an error function which is difficult to minimize because of numerous local minima [8]. The polynomial approximation of the projection function was introduced by Scaramuzza [9], who proposed a calibration toolbox for his model. The generic model, also known as the unified model, was introduced by Geyer [10] and Barreto [11], who proved its validity for all central catadioptric systems. This model was then modified by Mei, who generalized the projection matrix and also took into account the distortions (see [8] for more details). We chose to work with the unified model described by Mei (see Fig. 4) because any catadioptric system can be used and the number of parameters to be estimated is quite reasonable.

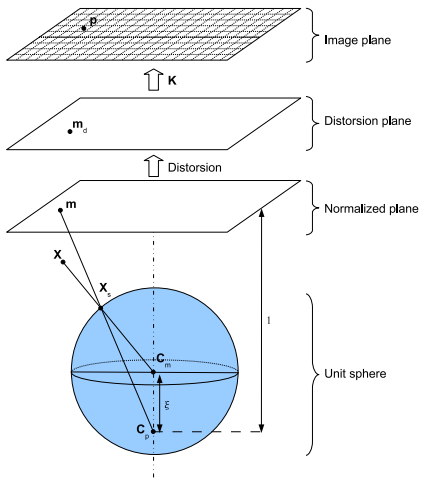

Fig. 4. Unified projection model.

A. Projection of a 3D point

A detailed description of the model can be found in [8]. The model contains 11 intrinsic parameters: one mirror parameter (ξ), 5 distortion parameters (k_1, k_2, k_3, k_4, k_5) and 5 parameters for the generalised camera projection matrix ($\alpha, \gamma_u, \gamma_v, u_0, v_0$). To summarize, the projection $\mathbf{p}$ of a 3D point $\mathbf{X}$ can be computed using the following steps (see Fig. 4):

- The world point $\mathbf{X}$ in the mirror frame is projected onto the unit sphere: $\mathbf{X} \rightarrow \mathbf{X}_S$
- This point is then changed to a new reference frame centered in $\mathbf{C}_p$
- It is then projected onto the normalized plane: $\mathbf{X}_S \rightarrow \mathbf{m}$
- Distortions are added: $\mathbf{m} \rightarrow \mathbf{m}_d$
- A perspective projection is then applied:

$$\mathbf{p} = \mathsf{K}\mathbf{m}_d = \begin{bmatrix} \gamma_u & \gamma_u\alpha & u_0 \\ 0 & \gamma_v & v_0 \\ 0 & 0 & 1 \end{bmatrix} \mathbf{m}_d \tag{1}$$

B. Lifting

The lifting step is the calculation of the point $\mathbf{X}_S$ on the unit sphere corresponding to a pixel, which is very useful for triangulation. Given $\mathbf{m} = [x\ y\ 1]^T$ the coordinates of the pixel on the normalized plane, we have:

$$\mathbf{X}_S = \begin{bmatrix} \frac{\xi+\sqrt{1+(1-\xi^2)(x^2+y^2)}}{x^2+y^2+1} x \\ \frac{\xi+\sqrt{1+(1-\xi^2)(x^2+y^2)}}{x^2+y^2+1} y \\ \frac{\xi+\sqrt{1+(1-\xi^2)(x^2+y^2)}}{x^2+y^2+1} - \xi \end{bmatrix} \tag{2}$$

IV. CALIBRATION

The calibration step is very easy to achieve because it only requires the catadioptric sensor to observe a planar pattern at different positions. The pattern can be freely moved (the motion does not need to be known) and the user only needs to select the four corners of the pattern.

The calibration process is similar to that of Christopher Mei [8]. It consists of a minimization over all the model parameters of an error function between the estimated projection of the pattern corners and the measured projection thanks to the Levenberg-Marquardt algorithm.

V. RELATIVE POSE ESTIMATION

Once the sensor calibration is completed, we have to know the relative pose of the two sensors to achieve a 3D reconstruction by triangulation. There are two ways to determine the relative pose of the two sensors : either by finding the essential matrix using the epipolar geometry then decomposing it to obtain the translation and the rotation between the two sensors, or by using a pattern to find the relative pose directly. Both methods have been implemented.

A. Essential matrix estimation using epipolar geometry

Epipolar geometry describes the relationship between two cameras. Since it depends only on the parameters of the cameras and their relative pose (it is independent of the scene structure), it can be computed from the correspondence of a few points. The main aim of determining the epipolar geometry is to compute the relative pose of the two sensors (or the displacement of one sensor) but it is also useful for simplifying the search for corresponding points in the two images.

Epipolar geometry is well-known for classical cameras [12] [13]. Given a point on the first image, a line on which the corresponding point lies on the second image can be determined. This line is known as an epipolar line and corresponds to the intersection of an epipolar plane with the image plane. Epipolar geometry of catadioptric sensors is more complicated because of the complex shape of the mirror. It is nevertheless possible to argue from analogy with a classical camera by working with points on the unit sphere (lifted points) rather than image points.

Let the projection of a 3D point $\mathbf{X}$ onto the unit spheres be denoted $\mathbf{X}_{S1}$ and $\mathbf{X}_{S2}$ (see Fig. 5), and R and $\mathbf{t}$ be the rotation and the translation between the two sensors. The coplanarity constraint of the points $\mathbf{X}$, $\mathbf{X}_{S1}$, $\mathbf{X}_{S2}$, $\mathbf{C}_1$ and $\mathbf{C}_2$ can be expressed as follows:

$$\mathbf{X}_{S2}\mathsf{R}(\mathbf{t} \wedge \mathbf{X}_{S1}) = 0 \tag{3}$$

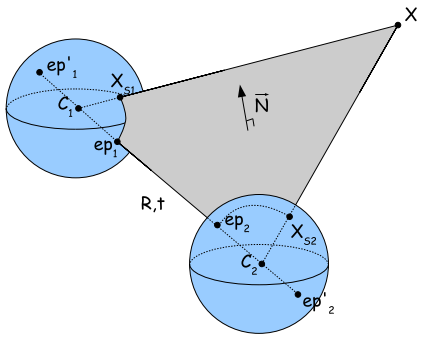

Fig. 5. Epipolar geometry of spherical sensors.

The coplanarity constraint (3) can be expressed in matrix form:

$$\mathbf{X}_{S2}^T \mathsf{E} \mathbf{X}_{S1} = 0 \tag{4}$$

where

$$\mathsf{E} = \mathsf{R}\mathsf{S} \tag{5}$$

is the essential matrix first introduced by Longuet-Higgins [14] and S is an antisymmetric matrix characterizing the translation: $\mathsf{S} = \begin{bmatrix} 0 & -t_z & t_y \\ t_z & 0 & -t_x \\ -t_y & t_x & 0 \end{bmatrix}$.

Given two lifted points $\mathbf{X}_{S1} = \begin{bmatrix} x_1 & y_1 & z_1 \end{bmatrix}^T$ and $\mathbf{X}_{S2} = \begin{bmatrix} x_2 & y_2 & z_2 \end{bmatrix}^T$ corresponding to the same 3D point $\mathbf{X}$, (4) becomes for each pair of matched points:

$$x_2x_1e_{11} + x_2y_1e_{12} + x_2z_1e_{13} + \cdots + z_2z_1e_{33} = 0 \quad (6)$$

where $\mathsf{E} = \begin{bmatrix} e_{11} & e_{12} & e_{13} \\ e_{21} & e_{22} & e_{23} \\ e_{31} & e_{32} & e_{33} \end{bmatrix}$.

With n matched points ($n \geq 8$), we can build a system of equations of the form [13]:

$$\mathsf{A}\mathbf{e} = 0 \quad (7)$$

where $\mathbf{e} = \begin{bmatrix} e_{11} & e_{12} & e_{13} & \cdots & e_{31} & e_{32} & e_{33} \end{bmatrix}^T$.

The essential matrix is computed through the following steps:

- detection of Harris corners
- matching of the corners with backward correlation in order to reject the false matches as described in [15]
- resolution of (7) by Singular Value Decomposition of A

B. Calibration with pattern

To plan its path, a robot must have a metric model of its environment, which implies knowledge of the baseline. Nevertheless, the essential matrix is estimated up to a scale factor with the eight-point algorithm [13], which leads only to a projective reconstruction. To solve this problem, we developed another method for the relative pose estimation problem.

This method uses patterns shown at different positions as with calibration. Let $\mathbf{X}$ be a point with coordinates $\mathbf{X}_1 = \begin{bmatrix} x_1 & y_1 & z_1 \end{bmatrix}^T$ in the first frame associated with the first sensor (see Fig. 6). Its coordinates in the second sensor reference frame can be expressed by:

$$\begin{bmatrix} x_2 \\ y_2 \\ z_2 \end{bmatrix} = \begin{bmatrix} r_{11} & r_{12} & r_{13} \\ r_{21} & r_{22} & r_{23} \\ r_{31} & r_{32} & r_{33} \end{bmatrix} \begin{bmatrix} x_1 \\ y_1 \\ z_1 \end{bmatrix} + \begin{bmatrix} t_x \\ t_y \\ t_z \end{bmatrix} \quad (8)$$

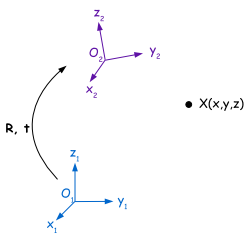

Fig. 6. Relative pose estimation principle.

With n control points, we can build the following system using (8):

$$\begin{bmatrix} x_1^1 & y_1^1 & z_1^1 & 0 & 0 & 0 & 0 & 0 & 0 & 1 & 0 & 0 \\ 0 & 0 & 0 & x_1^1 & y_1^1 & z_1^1 & 0 & 0 & 0 & 0 & 1 & 0 \\ 0 & 0 & 0 & 0 & 0 & 0 & x_1^1 & y_1^1 & z_1^1 & 0 & 0 & 1 \\ \vdots & \vdots & \vdots & \vdots & \vdots & \vdots & \vdots & \vdots & \vdots & \vdots & \vdots & \vdots \\ x_1^n & y_1^n & z_1^n & 0 & 0 & 0 & 0 & 0 & 0 & 1 & 0 & 0 \\ 0 & 0 & 0 & x_1^n & y_1^n & z_1^n & 0 & 0 & 0 & 0 & 1 & 0 \\ 0 & 0 & 0 & 0 & 0 & 0 & x_1^n & y_1^n & z_1^n & 0 & 0 & 1 \end{bmatrix} \begin{bmatrix} r_{11} \\ r_{12} \\ r_{13} \\ r_{21} \\ r_{22} \\ r_{23} \\ r_{31} \\ r_{32} \\ r_{33} \\ t_x \\ t_y \\ t_z \end{bmatrix} = \begin{bmatrix} x_2^1 \\ y_2^1 \\ z_2^1 \\ \vdots \\ x_2^n \\ y_2^n \\ z_2^n \end{bmatrix} \quad (9)$$

The 3D coordinates of the pattern corners are estimated using the Levenberg-Marquardt algorithm. The resolution of (9) gives the relative pose (R, $\mathbf{t}$) of the two sensors including the scale factor.

Once the relative pose is computed, the essential matrix can be easily computed thanks to (5).

VI. 3D RECONSTRUCTION

Reconstruction consists in determining the 3D coordinates of a point $\mathbf{X}$, given its projections $\mathbf{x}_1$ and $\mathbf{x}_2$ onto the two images. Consequently, the first step is to match pixels.

A. Epipolar geometry helps pixel matching

In addition to the essential matrix estimation, epipolar geometry possesses some helpful properties for pixel matching.

For each point $\mathbf{X}_{S1}$ on the first unit sphere, the epipolar curve is characterized by the normal of the plane $\mathbf{n}_2 = \mathsf{E}\mathbf{X}_{S1}$. The epipolar curve on the second image is obtained by determining the intersection of the plane and the second equivalence sphere, which is a great circle. In the same way, $\mathbf{n}_1 = \mathsf{E}^T\mathbf{X}_{S2}$ characterizes the epipolar curve corresponding to $\mathbf{X}_{S2}$ on the second sphere.

The epipoles are the points of intersection of the line joining the center with the unit sphere. All the epipolar curves intersect at the two epipoles. They can be directly computed from the essential matrix by singular value decomposition as in the classical case [13].

B. Mid-point method

In theory, the rays corresponding to two matched pixels must intersect at $\mathbf{X}$. In practice, however, various types of noise (distortions, small errors in the model parameters, etc) lead to lines generated by corresponding image points which do not always intersect. The problem is to find a 3D point which optimally fits the measured image points [13].

This step is achieved by using the mid-point method (see Fig. 7). Lifted points $\mathbf{X}_{S1}$ and $\mathbf{X}_{S2}$ corresponding to the pixels are first computed using (2). These points are then used to define the direction vectors $\mathbf{v}_1$ and $\mathbf{v}_2$ of the two rays. The 3D point $\mathbf{X}$ is chosen as the mid-point of the shortest transversal between the two rays.

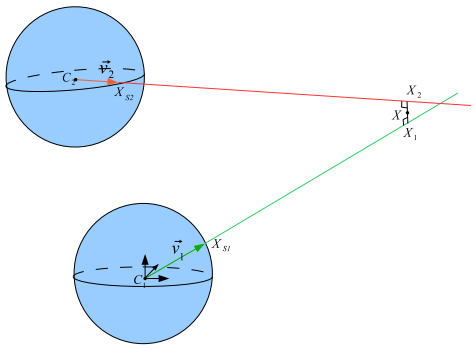

Fig. 7. Mid-point method. The 3D point **X** is chosen as the mid-point of the shortest transversal between the two rays.

VII. EXPERIMENTAL RESULTS

Each step of the 3D reconstruction was evaluated and a global result is shown at the end of this section. Experiments were implemented on real images and without prior knowledge to evaluate our system in real conditions.

A. Calibration

The calibration was evaluated by computing the Root of Mean Squares (RMS) distances (in pixels) between the extracted corners (77 per image) of the pattern and the reprojected ones. Figure 8 shows the RMS error with respect to the number of images of the pattern used for the calibration. We can notice that the error decreases when more images are used but tends to stabilize from 6 images. The minimum RMS value obtained is then about 0.02 pixels.

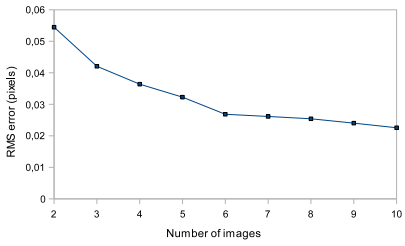

Fig. 8. RMS error versus the number of images of the pattern.

The model parameters obtained by the calibration allows the lifting, i.e. the projection of the pixels onto the unit sphere as shown in Figure 9.

B. Relative pose estimation

The relative pose estimation was evaluated on real images. The sensor was mounted on a graduated rail and was moved 10cm by 10cm. At each position, an omnidirectional image was acquired with the aim of computing the displacement of the sensor according to the first position using five calibration patterns placed in the room (see Fig. 10).

Table I summarizes the results. The average error is less than 0.9%.

Fig. 9. An omnidirectional image and two views of its projection onto the unit sphere.

Displacement (mm)	100	200	300	400	500	600
Estimation (mm)	100.13	200.77	296.48	393.66	494.70	594.60

TABLE I
ESTIMATION OF THE DISPLACEMENTS

Once the relative pose is estimated, we can compute the essential matrix and use it to check epipolar geometry properties. In figure 10, for each selected pixel on the left image (red crosses), the corresponding epipolar curve (green curves) is drawn on the right image and vice versa.

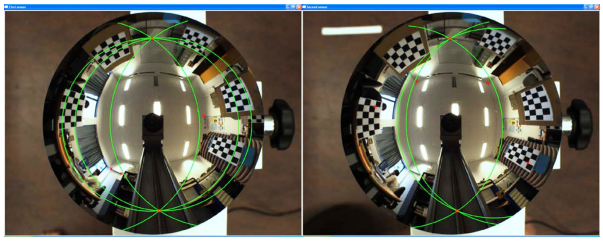

Fig. 10. Epipolar curves (green) corresponding to selected pixels (red crosses).

C. 3D reconstruction

The entire process was evaluated by a piecewise planar 3D reconstruction of our laboratory (see Fig. 11). The four corners of the ceiling were manually selected to check the size of the room. After triangulation, we estimated the ceiling dimension at 6.39 x 6.34 meters and the actual size is 6.4 x 6.4 m.

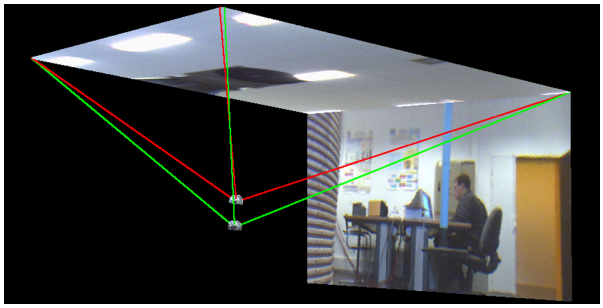

Fig. 11. Piecewise planar 3D reconstruction of our laboratory.

VIII. DISCUSSION

In this paper, we have used a stereovision system based on two catadioptric sensors (see Fig. 1) mounted co-axially one above the other. Indeed, such a configuration greatly simplifies the epipolar geometry since epipolar curves become radial lines. By this way, matching horizontal lines is simplified while a motion allows vertical lines to be matched. A stereoscopic system also presents advantages compared to a structure from motion method because the baseline is well-known and not estimated by odometry which introduces many errors.

We have chosen to work with a unified model which is valid for all central sensors hence we have to respect the Single-Viewpoint constraint. Our method, presented in section 2, allows us to be as near as possible to the single viewpoint. The choice of the Mei's unified model leads to a very flexible calibration step because the number of parameters to be estimated is quite reasonable and easy to be initialized. A calibration tool was developed in C++ using the computer vision library OpenCV and can be freely downloaded from our website [16]. The calibration tool does not require any commercial software and optimizes the computing time. A calibration with 10 images does not exceed 2 minutes.

Two methods have been developed for the relative pose estimation and have different fields of use. The first one relies on the eight-point algorithm and can be used in line because the process is entirely automatic but gives only the relative pose up to a scale factor. The other one uses calibration patterns and is more adapted for measurement thanks to the entire knowledge of the relative pose. Table II summarizes the main characteristics of the two methods used for the relative pose estimation and their field of use. The evaluation of our method

	Eight-point algorithm	**Estimation with pattern**
Input data	a pair of omnidirectionnal images	pairs of omnidirectionnal images with a calibration pattern
Hypothesis on data	n points correctly matched	pattern properties known (size and number of squares), model parameters
Output data	essential matrix which can be decomposed into relative pose up to a scale factor	relative pose, the essential matrix can be easily computed from it
Error source	false matching	pattern position estimation
Computing time	long because of the pixels matching	short
Manipulation time	short (automatic process)	long (manual selection of the four corners of the pattern)
Field of use	*in line* calibration	*Off line* calibration

TABLE II

COMPARISON OF THE TWO RELATIVE POSE ESTIMATION METHODS.

using calibration patterns was done by estimating the motion of the sensor. The average error between estimation and real displacements is small (less than 2%) and probably induced by image noise which disturbs the corner extraction process. The precision is sufficient for applications such as navigation.

The piecewise planar 3D reconstruction is introduced for the validation of the calibration and triangulation steps. The good results obtained imply the reliable estimation of the parameters. The 3D reconstruction was done on manually selected points to avoid possible errors due to an automatic matching.

IX. CONCLUSION

In this paper, we have presented a scheme for 3D reconstruction of the environment of a mobile robot based on a catadioptric stereovision sensor. This scheme can be decomposed into three stages : calibration, estimation of the relative pose of the two sensors and triangulation.

Thanks to an accurate calibration and relative pose estimation, the metric of the scene is well respected and evaluated using real images.

Our future work will focus on automatic reconstruction, thanks to pixel matching or more elaborated primitives (lines, planes, etc). Once 3D reconstruction is achieved, the motion estimation of the robot will be addressed to be able to merge several local reconstructions.

ACKNOWLEDGMENT

This research is supported by the DGA (Délégation Générale pour l'Armement), IPSIS (Ingénierie pour Signaux et Systèmes) and IRSEEM (Institut de Recherche en Systèmes Electroniques Embarqués).

[1] R. Benosman and J. Devars, "Panoramic stereovision sensor," in *Int. Conf. on Pattern Recognition (ICPR'98)*, vol. 1, 1998, pp. 767–769.
[2] S. Baker and S. Nayar, "A theory of single-viewpoint catadioptric image formation," *Int. J. Comput. Vision*, vol. 35, no. 2, pp. 175–196, 1999.
[3] E. Mouaddib, "Introduction à la vision panoramique catadioptrique," *Trait. Signal*, vol. 22, no. 5, pp. 409–417, 2005.
[4] J. Bouguet, "Jean-yves bouguet's www homepage." [Online]. Available: http://www.vision.caltech.edu/bouguetj/
[5] S. Ramalingram, P. Sturm, and S. Lodha, "Towards complete generic camera calibration," in *Computer Vision and Pattern Recognition (CVPR'05)*, 2005, pp. 1093–1098.
[6] N. Ragot, J. Ertaud, X. Savatier, and B. Mazari, "Calibration of a panoramic stereovision sensor : Analytical vs interpolation-based methods," in *Industrial Electronics Conf. (IECON'06)*, 2006, pp. 4130–4135.
[7] J. Gonzalez-Barbosa and S. Lacroix, "Fast dense panoramic stereovision," in *Int. Conf. on Robotics and Automation (ICRA'05)*, 2005, pp. 1210– 1215.
[8] C. Mei and P. Rives, "Single view point omnidirectional camera calibration from planar grids," in *Int. Conf. on Robotics and Automation (ICRA'07)*, 2007, pp. 3945–3950.
[9] D. Scaramuzza, A. Martinelli, and R. Siegwart, "A flexible technique for accurate omnidirectional camera calibration and structure from motion," in *Int. Conf. on Computer Vision Systems (ICVS'06)*, 2006, pp. 45–52.
[10] C. Geyer and K. Daniilidis, "A unifying theory for central panoramic systems and practical implications," in *Eur. Conf. on Computer Vision (ECCV'00)*, 2000, pp. 445–461.
[11] J. P. Barreto, "A unifying geometric representation for central projection systems," *Comput. Vis. Image Underst.*, vol. 103, no. 3, pp. 208–217, 2006.
[12] Z. Zhang, "Determining the epipolar geometry and its uncertainty: A review," *Int. J. Comput. Vision*, vol. 27, no. 2, pp. 161–195, 1998.
[13] R. Hartley and A. Zisserman, *Multiple View Geometry in Computer Vision*, 2nd ed. Cambridge University Press, ISBN: 0521540518, 2004.
[14] H. Longuet-Higgins, "A computer algorithm for reconstructing a scene from two projections," *Nature*, vol. 293, pp. 133–135, 1981.
[15] P. Werth and S. Scherer, "A novel bidirectional framework for control and refinement of areabased correlation techniques," in *Int. Conf. on Pattern Recognition (ICPR'00)*, vol. 3, 2000, pp. 730–733.
[16] R. Boutteau, "3d reconstruction for autonomous navigation." [Online]. Available: http://omni3d.esigelec.fr/doku.php/thesis/r3d/start